JOURNAL OF SOLID STATE CHEMISTRY 54, 156–163 (1984)

Low-Temperature Luminescence of Eu^{3+} in K_2EuCl_5

HARRY G. BRITTAIN*

Department of Chemistry, Seton Hall University,
South Orange, New Jersey 07079

AND GERD MEYER

Institut für Anorganische und Analytische Chemie, Justus-Liebig
Universität, Heinrich-Buff-Ring 58, 6300 Giessen, West Germany

Received March 12, 1984

The luminescence associated with the Eu^{3+} ion in K_2EuCl_5 has been studied at cryogenic temperatures under conditions of high resolution. Emission was observed to originate from both the $^5D_0$ and $^5D_1$ excited states, and transitions to the $^7F_0$, $^7F_1$, $^7F_2$, $^7F_3$, and $^7F_4$ ground levels were observed. The fine structure observed within these emission bands was found to be consistent with the existence of an effective C_4 site symmetry for the emitting Eu(III) species, even though the crystal structure does not indicate the presence of a true or pseudo C_4 axis.

Introduction

The luminescence spectroscopy of lanthanide chloride complexes has been extensively studied in the past, and the results of these investigations have been used to deduce energy level patterns, details of the crystal field interactions, and to provide insight into the intensity mechanisms of these transitions. The Eu^{3+} ion is unique in that its lowest excited state is characterized by $J = 0$, and hence the luminescence spectroscopy of Eu^{3+} complexes is far easier to interpret than that of any other lanthanide ion. An extensive literature now exists concerning the emission spectroscopy of Eu^{3+} doped into hexagonal ($P6_3/m$) $LaCl_3$ (*1*), or cubic ($Pa3$) systems isomorphous with elpasonite (K_2NaAlF_6) (*2*). Recently the data obtained in these systems has been assembled into a compendium (*3*).

Far less work has been carried out detailing the luminescence spectra of Eu^{3+} chloro complexes in environments characterized by lower metal ion site symmetries. This observation is surprising considering the known chemistry of complex lanthanide halides (*4*). Recently, Meyer and Hüttl reported the crystal structure of K_2PrCl_5 (*5*), and noted that K_2EuCl_5 was isostructural with the Pr^{3+} salt. In this structure, the lanthanide ions were found to be 7-coordinate, and the coordination polyhedron was described as that of a monocapped trigonal prism.

In the present work, results of studies on the electronic structure of Eu^{3+} in K_2EuCl_5 are reported. The luminescence data which

---

* To whom correspondence should be addressed.

0022-4596/84 $3.00

will be reported were all obtained at cryogenic temperatures under conditions of high resolution.

Experimental

K_2EuCl_5 was prepared in a manner which has been described previously (*5*, *6*). The crystals used for the spectroscopic studies were taken from the very same batch which had been used for the crystallographic work. The cell constants for K_2EuCl_5 were found to be $a = 12.466$ Å, $b = 8.650$ Å, and $c = 7.942$ Å, and the molar volume was determined as 130.98 cm^3/mole (*5*). K_2EuCl_5 may be prepared by reacting $EuCl_3$ and KCl in a 1 : 2 mole ratio at 450°C for 1–2 days. The salt was stored under a dry argon atmosphere, and all spectral measurements were carried out under vacuum.

The room temperature excitation spectrum of K_2EuCl_5 was obtained at 2-Å resolution on a Spex Fluorolog spectrometer. All luminescence spectra were obtained on a high-resolution emission spectrometer constructed in our laboratory. Samples were excited by the 350-nm output (50 mW) of an Ar-ion laser, and the emission was analyzed at 2-cm^{-1} resolution by a 1-m grating monochromator (Spex Model 1704). The emission was detected by a cooled photomultiplier tube (S-20 response), and processed through the Spex digital photometer. In most work, the sample temperature was held between 8.5 and 9.0°K, with the low excitation power being desirable in that sample heating could be minimized. The K_2EuCl_5 sample was mounted on a Cu block bolted onto the cold stage of a closed-cycle cryogenic refrigator system (Lake Shore Cryotronics Model LTS-21). Data were also obtained at room temperature for comparison purposes.

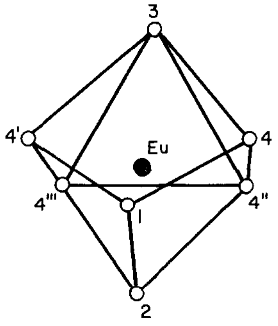

FIG. 1. Structure of the $[EuCl_7]$ polyhedra within the K_2EuCl_5 material. The structure is isomorphous with that reported for K_2PrCl_5 (*5*).

Results and Discussion

The Eu^{3+} polyhedron in K_2EuCl_5 may be described as a monocapped trigonal prism, in the *Pnma* space group (*5*). These prisms are built up into chains through a sharing of common edges in the (010) direction, as has been illustrated in Fig. 1 of Ref. (*5*). In the ideal monocapped trigonal prismatic symmetry, the Eu^{3+} ion would occupy a site of C_{2v} symmetry (*7*). However, the difference between the monocapped trigonal prism and the monocapped octahedron is not great, and the distinction between the two polyhedra is somewhat arbitrary in the case of K_2EuCl_5. The idealized point group associated with a monocapped octahedron would be C_{3v} (*7*).

The difficulty associated with assigning a particular polyhedron to $[EuCl_7]^{2-}$ is evident through consideration of the crystal structure of the isomorphous K_2PrCl_5 compound (*5*), as has been illustrated in Fig. 1. If one considers the $[PrCl_7]$ unit as 3 : 4 polyhedron, then it would have 12 edges: Cl(1)–Cl(2) [3.409 Å], Cl(1)–Cl(4)/Cl(1)–Cl(4′) [3.430 Å], Cl(2)–Cl(4′)/Cl(2)–Cl(4‴) [3.592 Å], Cl(3)–Cl(4)/Cl(3)–Cl(4′) [3.718 Å], Cl(3)–Cl(4″)/Cl(3)–Cl(4‴) [3.758 Å], Cl(4)–Cl(4″)/Cl(4)–Cl(4′) [3.389 Å], and Cl(4)/Cl(4′) [3.611 Å]. The capped octahedron has 13 edges, consisting of the former 12 plus Cl(4″)–Cl(4‴) [5.145 Å]. Accompanied with that large distance is a dihedral angle for the Cl(4)–Cl(4″)/Cl(4′)–Cl(4‴)

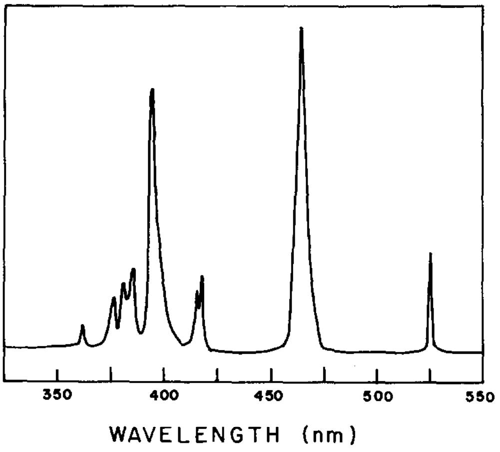

FIG. 2. Room-temperature excitation spectrum of the Eu(III) ion in K_2EuCl_5. An emission wavelength of 613 nm was used in the determination.

plane of 156.8° (instead of 180°). Cl(1), Cl(2), and Cl(3) lie within a mirror plane, so that Cl(4)/Cl(4′) and Cl(4″)/Cl(4‴) are crystallographically equivalent. The angle Cl(1)–Pr–Cl(2) is only 75.4°, and therefore the Cl(2)–Pr–Cl(3) angle is 158.3° and the Cl(1)–Pr–Cl(3) angle is 126.3°.

The room temperature excitation spectrum of K_2EuCl_5 is shown in Fig. 2. Assignment of the various peaks was carried out using the known free ion values of the Eu^{3+} ion (*8*), and these assignments may be found in Table I. The energies of the excited states found for Eu^{3+} in K_2EuCl_5 were observed to be very close to those noted for Eu^{3+} doped into $LaCl_3$ (*1*). While the major excitation bands of the Eu^{3+} happened not to coincide with the uv output of the Ar-ion laser, sufficient absorption existed at 350 nm to permit the performance of luminescence studies on the K_2EuCl_5 complex.

Luminescence was found to originate from both the $^5D_0$ and $^5D_1$ excited states, and this behavior was noted both at room and cryogenic temperatures. The emission was actually found to be fairly intense, indicating a relatively low degree of concentration quenching in the K_2EuCl_5 system. A sequence of transitions to the various ^7F_J levels of the ground state was observed, the identity of which was obvious after a comparison with the free ion values (*8*). Experimental constraints limited our investigations to transitions terminating in the ^7F_J levels characterized by $J = 0, 1, 2, 3$, or 4. For the sake of simplicity, we will henceforth refer to the various *f–f* transitions by their defining *J* quantum numbers.

As may be seen in Figs. 3–9, each luminescent transition contains a wealth of fine

TABLE I

ENERGY LEVELS OF THE VARIOUS Eu(III) STATES IN K_2EuCl_5 AS DEDUCED FROM THE EXCITATION SPECTRUM

Wavelength (nm)	Energy (cm^{-1})	Assignment
581	17,220	$^5D_0$
527	18,980	$^5D_1$
465	21,510	$^5D_2$
418	23,920	$^5D_3$
395	25,320	$^5L_6$
386	25,910	$^5L_7$
381	26,250	$^5G_{2,3,4}$
377	26,530	
362	27,620	$^5D_4$

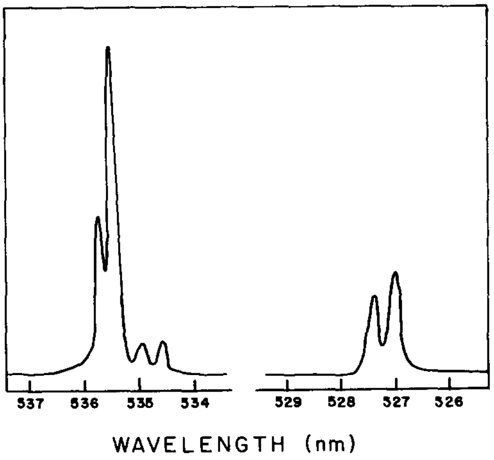

FIG. 3. Luminescence spectra of the $^5D_1 \rightarrow {}^7F_0$ and $^5D_1 \rightarrow {}^7F_1$ transitions of Eu(III) in K_2EuCl_5, obtained at 9.0 K. The 1–0 band system is located at shorter wavelengths relative to the 1–1 system.

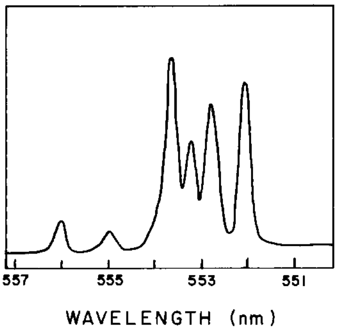

FIG. 4. Luminescence spectrum of the $^5D_1 \rightarrow {}^7F_2$ transition of Eu(III) in K_2EuCl_5, obtained at 9.0 K.

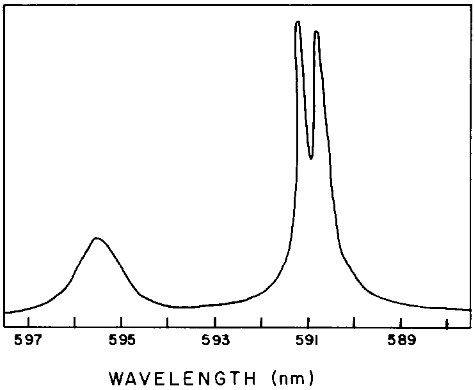

FIG. 6. Luminescence spectrum of the $^5D_0 \rightarrow {}^7F_1$ transition of Eu(III) in K_2EuCl_5, obtained at 9.0 K.

structure, and is found to occur in a characteristic spectral region. None of the $^5D_J \rightarrow {}^7F_J$ transitions overlaps to any significant extent with any other emission band. Several band systems were found to contain a few sharp peaks at high energy, followed by significantly broader bands at slightly lower energies. This behavior suggests that the broad bands are vibronic in nature, and that only the sharp peaks correspond to the true electronic transitions. These transitions will certainly contain electric dipole character, as the Eu^{3+} ion does not reside in a high-symmetry site. A tabulation of the wavelengths and energies corresponding to all major peaks may be found in Table II. No data could be reported for the 1–4 transition, as these bands were obscured by the intense 0–2 band system.

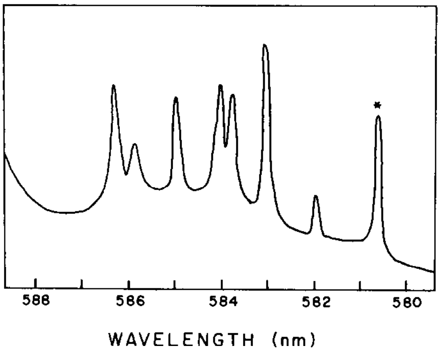

FIG. 5. Luminescence spectra of the $^5D_0 \rightarrow {}^7F_0$ and $^5D_1 \rightarrow {}^7F_3$ transitions of Eu(III) in K_2EuCl_5, obtained at 9.0 K. The sole 0–0 peak has been marked by the asterisk.

No crystal field is capable of splitting the nondegenerate levels corresponding to $J = 0$. Consequently, transitions from the $^5D_0$ and $^5D_1$ emitting states to the $^7F_0$ ground level are particularly useful in locating the energies of any and all emitting levels. The number of crystal field components associated with the $^5D_1$ excited state will equal the number of peaks observed within the 1–0 band system. Two peaks were found within the 1–0 band envelope (19,000 and 18,971 cm^{-1}), and hence we conclude that the D emitting state is split into two crystal field

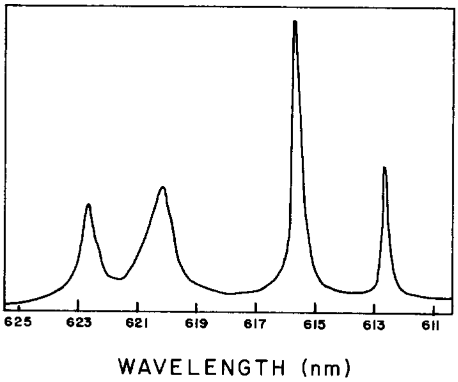

FIG. 7. Luminescence spectrum of the $^5D_0 \rightarrow {}^7F_2$ transition of Eu(III) in K_2EuCl_5, obtained at 9.0 K.

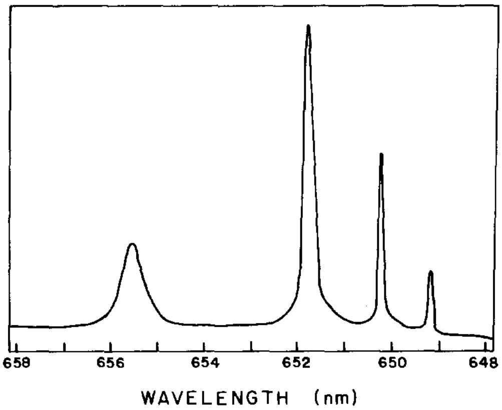

FIG. 8. Luminescence spectrum of the $^5D_0 \rightarrow {}^7F_3$ transition of Eu(III) in K_2EuCl_5, obtained at 9.0 K.

states. The 0–0 transition was found to yield a single weak band at 17,222 cm^{-1}, and of course this transition cannot be split by any crystal field.

The $^5D_0$ level is thus the origin associated with each of the 0–J transitions, and each component of the $^5D_1$ level may be considered as an origin for the 1–J transitions. Each peak reported in Table II may thus be assigned as a transition from one of these three origins to the crystal field components

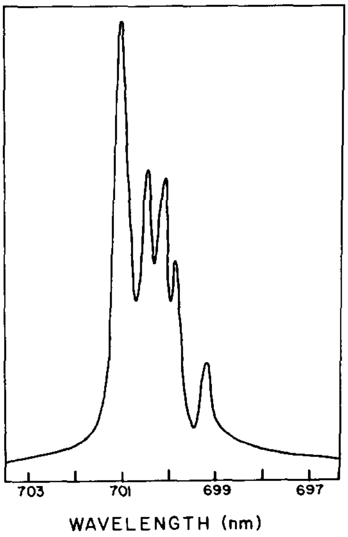

FIG. 9. Luminescence spectrum of the $^5D_0 \rightarrow {}^7F_4$ transition of Eu(III) in K_2EuCl_5, obtained at 9.0 K.

TABLE II

WAVELENGTHS, ENERGIES, AND ASSIGNMENTS FOR THE VARIOUS Eu(III) EMISSION BANDS AS OBTAINED IN K_2EuCl_5

Wavelength (Å)	Energy (cm^{-1})	Assignment [$J(i) \rightarrow J(i')$]
1–0 Band		
5263	19,000	1(b)–0(a)
5271	18,971	1(a)–0(a)
1–1 Band		
5346	18,707	1(b)–1(a)
5350	18,692	1(b)–1(b)
5354	18,678	1(a)–1(a)
5357	18,668	1(a)–1(b)
1–2 Band		
5520	18,117	1(a)–2(a)
5528	18,091	1(b)–2(c)
5532	18,078	1(a)–2(b)
5535	18,067	1(a)–2(c)
5549	18,022	1(b)–2(d)
5560	17,987	1(a)–2(d)
0–0 Band		
5807	17,222	0(a)–0(a)
1–3 Band		
5820	17,183	1(b)–3(a)
5830	17,153	1(a)–3(a) + 1(b)–3(b)
5837	17,132	1(a)–3(b)
5839	17,125	1(b)–3(c)
5849	17,097	1(a)–3(c)
5859	17,068	1(a)–3(d)
5864	17,053	1(a)–3(e)
0–1 Band		
5908	16,927	0(a)–1(a)
5912	16,916	0(a)–1(b)
5955	16,791	Vibronic
0–2 Band		
6127	16,321	0(a)–2(c)
6157	16,243	0(a)–2(d)
6202	16,125	Vibronic
6228	16,056	Vibronic
0–3 Band		
6492	15,405	0(a)–3(a)
6502	15,380	0(a)–3(b)
6518	15,343	0(a)–3(c)
0–4 Band		
6992	14,303	0(a)–4(a)
6998	14,290	0(a)–4(b)
7000	14,285	0(a)–a(c)
7003	14,279	0(a)–4(d)
7009	14,266	0(a)–4(e)

of each ^7F_J state. The actual number of peaks observed within a give band system depends on the site symmetry of the emitting Eu(III) ion. Forsberg (*9*) has tabulated the selection rules for the 0–J transitions as would exist in any noncentrosymmetric point group.

Should the Eu^{3+} ion actually reside at a site characterized by C_{2v} symmetry (equivalent to the holohedrized symmetry), then the state splitting induced by the crystal field would lead to the observation of one 0–0 peak, two 0–1 peaks, four 0–2 peaks, five 0–3 peaks, and seven 0–4 peaks. If none of the 0–2 peaks were vibronic in nature, then C_{2v} symmetry would certainly agree with the 0–0, 0–1, and 0–2 data. However, only three peaks were found in the 0–3 band region, and only five peaks were observed for the 0–4 transition. These observations indicate that as far as spectroscopic requirements go, the effective site symmetry of the Eu^{3+} ion in K_2EuCl_5 cannot be taken as C_{2v}.

Comparison of the observed 0–J patterns with those predicted by Forsberg (*9*) reveals that only one possible site symmetry fits the observed data. Were the Eu^{3+} ion to experience C_4 symmetry through some mechanism, then the observed spectrum would consist of one 0–0 peak, two 0–1 peaks, two 0–2 peaks, three 0–3 peaks, and five 0–4 peaks. If the broad 0–1 peak (found at 5955 Å) and the broad 0–2 peaks (located at 6202 and 6228 Å) were indeed vibronic in nature, then the observed peak pattern would perfectly match that predicted on the basis of C_4 symmetry.

The entire emission sequence associated with the transitions out of the $^5D_1$ excited state cannot be made to agree with the existence of C_{2v} symmetry. However, the assumption of C_4 symmetry *does* permit a complete explanation of the fine structure observed within the 1–0, 1–1, 1–2, and 1–3 band systems. In C_4 symmetry, one finds that the various J-states split according to the scheme:

$$
\begin{array}{ll}
J = 0, & A \\
J = 1, & A + E \\
J = 2, & A + 2B + E \\
J = 3, & A + 2B + 2E \\
J = 4, & 3A + 2B + 2E.
\end{array}
$$

The selection rules corresponding to the 0–J transitions may be obtained from the literature (*9*), and in Table III the selection rules governing emission out of the $^5D_1$ excited state have been detailed.

The $^5D_1$ state is thus predicted to split into $A + E$ components, and one would anticipate that emission out of both crystal field components ought to occur. Two transitions are possible within the 1–0 band system, and both are allowed in C_4 symmetry. The transitions out of the 18,971-cm^{-1} level are normally found to be more intense than

TABLE III

ELECTRIC DIPOLE SELECTION RULES GOVERNING THE $^5D_1 \rightarrow {}^7F_J$ LUMINESCENT TRANSITIONS IN C_4 SYMMETRY

	Excited state	
Transition	*A* symmetry	*E* symmetry
$1 \rightarrow 0$		
A	+	+
$1 \rightarrow 1$		
A	+	+
E	+	+
$1 \rightarrow 2$		
A	+	+
2 *B*	–	+
E	+	+
$1 \rightarrow 3$		
A	+	+
2 *B*	–	+
2 *E*	+	+
$1 \rightarrow 4$		
3 *A*	+	+
2 *B*	–	+
2 *E*	+	+

Note. An allowed transition is indicated by (+), while a forbidden transition is denoted by (–).

the corresponding transitions out of the 19,000 cm^{-1} level. This would indicate that thermal equilibration within the $^5D_1$ level is taking place, and hence the lower crystal field component is more populated. A comparison of the predicted number of allowed electric dipole transitions with the observed number of 1–J transitions reveals that in every case, the theoretical prediction agrees with the experimental result. It should be noted that only the assumption of C_4 symmetry enables one to completely fit all the observed 1–J transitions.

One may use the data of Table II to calculate the energies corresponding to the crystal field substates of the ^5D_J and ^7F_J levels, and these are located in Table IV. In this process, we have assumed that the energy of the $^7F_0$ level equals zero.

Assignment of the symmetries associated with each level is more difficult. For the 0–J transitions, only the $A \rightarrow A$ and $A \rightarrow E$ transitions can be observed. This property allows one to determine the energies of the A and E components of the ^7F_J levels. It is not possible at this time to provide a definitive assignment regarding whether a given level has either A or E symmetry, but at least one can rule out B symmetry.

Comparison of the data present in Table II with the selection rules of Table III permits a facile assignment of the symmetry labels associated with the two components of the $^5D_1$ excited state. In the 1–J band systems, emission from the 18,971-cm^{-1} level to every ^7F_J level is observed. In several instances, anticipated transitions from the 19,000-cm^{-1} level were not seen. According to the C_4 selection rules, the $E \rightarrow A$, $E \rightarrow B$, and $E \rightarrow E$ transitions are all allowed. On the other hand, the $A \rightarrow B$ transition is forbidden by group theory, and only the $A \rightarrow A$ and $A \rightarrow E$ transitions are allowed. It is therefore clear that the 18,971-cm^{-1} level of the $^5D_1$ excited state is of E symmetry, while the 19,000-cm^{-1} level is of A symmetry. The $E \rightarrow A,B,E$ transitions which have no counterpart in the $A \rightarrow A,E$ sequences serve to identify the ^7F_J levels characterized by B symmetry. While the ^7F_J levels which possess B symmetry are readily identified, it is still not possible to provide definitive symmetry labels for the other ^7F_J levels.

It is an apparent contradiction that the spectroscopy of the Eu(III) ion in the K_2EuCl_5 system can be described quite well by the assumption of a C_4 site symmetry for this ion. Examination of the crystal struc-

TABLE IV

ENERGIES OF THE VARIOUS CRYSTAL FIELD COMPONENTS OF THE Eu(III) STATES IN K_2EuCl_5 AS DEDUCED FROM THE LUMINESCENCE SPECTRA

State	Energy (cm^{-1})	Symmetry
$^7F_0$ Level		
(a)	0	A
$^7F_1$ Level		
(a)	295	A/E
(b)	306	A/E
$^7F_2$ Level		
(a)	854	B
(b)	893	B
(c)	901	A/E
(d)	979	A/E
$^7F_3$ Level		
(a)	1817	A/E
(b)	1842	A/E
(c)	1879	A/E
(d)	1904	B
(e)	1913	B
$^7F_4$ Level		
(a)	2919	A/E
(b)	2932	A/E
(c)	2937	A/E
(d)	2943	A/E
(e)	2956	A/E
(f)	*	B
(g)	*	B
$^5D_0$ Level		
(a)	17,222	A
$^5D_1$ Level		
(a)	18,971	E
(b)	19,000	A

Note. The * indicates that a transition to this level was not observed.

ture reveals only the existence of a mirror plane within the Eu^{3+} coordination polyhedron. No indication of a true or pseudo C_4 axis can be deduced from consideration of the structure. This situation indicates that the observed spectra must contain either accidental degeneracies, or that transitions to certain crystal field components were too weak to be observed.

Acknowledgments

This work was supported by the Camille and Henry Dreyfus Foundation, through a Teacher-Scholar award to HGB, and by a grant from the Deutsche Forschungsgemeinschaft, Bonn, to GM.

References

1. G. H. Dieke, "Spectra and Energy Levels of Rare Earth Ions in Crystals." Interscience, New York (1968).
2. (a) O. A. Serra and L. C. Thompson, *Inorg. Chem.* **15,** 504 (1976); (b) C. D. Flint and F. L. Stewart-Darling, *Mol. Phys.* **44,** 61 (1981); (c) J. P. Morley, T. R. Faulkner, and F. S. Richardson, *J. Chem. Phys.* **77,** 1710 (1982).
3. C. A. Morrison and R. P. Leavitt, *in* "Handbook on the Physics and Chemistry of Rare Earths" (K. A. Gschneider, Jr. and L. Eyring, Eds.), Chap. 46, North-Holland, Amsterdam (1982).
4. G. Meyer, *Prog. Solid State Chem.* **14,** 141 (1982).
5. G. Meyer and E. Hüttl, *Z. Anorg. Allg. Chem.* **497,** 191 (1983).
6. G. Meyer, *Inorg. Synth.* **22,** 1 (1983).
7. S. P. Sinha, *Struct. Bonding* **25,** 69 (1976).
8. G. S. Ofelt, *J. Chem. Phys.* **38,** 2171 (1963).
9. J. H. Forsberg, *Coord. Chem. Rev.* **10,** 195 (1973).